We are IntechOpen, the world's leading publisher of Open Access books
Built by scientists, for scientists

6,900
Open access books available

186,000
International authors and editors

200M
Downloads

154
Countries delivered to

Our authors are among the

TOP 1%
most cited scientists

12.2%
Contributors from top 500 universities

CLARIVATE ANALYTICS
BOOK CITATION INDEX
INDEXED

WEB OF SCIENCE™

Selection of our books indexed in the Book Citation Index
in Web of Science™ Core Collection (BKCI)

Interested in publishing with us?
Contact book.department@intechopen.com

Numbers displayed above are based on latest data collected.
For more information visit www.intechopen.com

Fuzzy Logic Control of a Smart Actuation System in a Morphing Wing

Teodor Lucian Grigorie, Ruxandra Mihaela Botez and Andrei Vladimir Popov

Additional information is available at the end of the chapter

1. Introduction

The actual trends in aerospace engineering are related to the green aircrafts development and to theirs' constructive parts optimization in order to obtain important fuel and energy savings. A lot of these studies refer to the aircrafts' shape optimization, taking into account that the aircraft drag force influences directly the fuel consumption. In this way, a very interesting and provocative concept was launched on the market, i.e. "morphing aircraft". Considering the drag reduction, fuel consumption economy and flight envelope increasing promising benefits, many universities, R&D institutions and industry initiated and developed morphing aircrafts studies in the last decade (Munday and Jacob, 2002; Sanders, 2003; Manzo et al., 2004; Skillen and Crossley, 2005; Bornengo et al., 2005; Moorhouse et al., 2006; Namgoong et al., 2006; Namgoong et al., 2007; Seigler et al., 2007; Obradovic and Subbarao, 2011 a; Obradovic and Subbarao, 2011 b; Gamboa et al., 2009; Baldelli at al., 2008; Inoyama et al., 2008; Thill et al., 2008; Perera and Guo, 2009; Bilgen et al., 2009; Bilgen et al., 2010; Thill et al., 2010; Seber and Sakarya, 2010; Wildschek et al., 2010; Ahmed et al., 2011). The multidisciplinary aspects involved by such studies, bring together research teams in many fields of the science: aerodynamics and aeroelasticity, automation, electrical engineering, materials engineering, control and software engineering. Categorized as a part of the "Smart structures" engineering field, the general concept of morphing aircrafts includes some particular elements, as a function by the complexity of the developed morphing application. Recent researches in smart materials and adaptive structures fields have led to a new way to obtain a morphing aircraft by changing the shape of its wings through the control of the airfoils cambers; the concept was called "morphing wing". Therefore, a lot of architecture were and are still imagined, designed, studied and developed, for this new concept application. One of these is our team project including the numerical simulations and experimental multidisciplinary studies using the wind tunnel for a morphing wing equipped with a flexible skin, smart

material actuators and pressure sensors. The aim of these studies is to develop an automatic system that, based on the information related to the pressure distribution along the wing chord, moves the transition point from the laminar to the turbulent regime closer to the trailing edge in order to obtain a larger laminar flow region, and, as a consequence, a drag reduction.

The objective of the research presented here is to develop a new morphing mechanism using smart materials such as Shape Memory Alloy (SMA) as actuators and fuzzy logic techniques. These smart actuators deform the upper wing surface, made of a flexible skin, so that the laminar-to-turbulent transition point moves closer to the wing trailing edge. The ultimate goal of this research project is to achieve drag reduction as a function of flow condition by changing the wing shape. The transition location detection is based on pressure signals measured by optical and Kulite sensors installed on the upper wing flexible surface. Depending on the project evolution phase, two architectures are considered for the morphing system: open loop and closed loop. The difference between these two architectures is their use of the transition point as a feedback signal. This research work was a part of a morphing wing project developed by the Ecole de Technologie Supérieure in Montréal, Canada, in collaboration with the Ecole Polytechnique in Montréal and the Institute for Aerospace Research at the National Research Council Canada (IAR-NRC) (Brailovski et al., 2008; Coutu et al., 2007; Coutu et al., 2009; Georges et al., 2009; Grigorie & Botez, 2009; Grigorie & Botez, 2010; Grigorie et al., 2010 a; Grigorie et al., 2010 b; Grigorie et al., 2010 c; Popov et al., 2008 a; Popov et al., 2008 b; Popov et al., 2009 a; Popov et al., 2009 b; Popov et al., 2010 a; Popov et al., 2010 b; Popov et al., 2010 c; Sainmont et. al., 2009), initiated and financially supported by the following government and industry associations: the Consortium for Research and Innovation in Aerospace in Quebec (CRIAQ), the National Sciences and Engineering Research Council of Canada (NSERC), Bombardier Aerospace, Thales Avionics, and the National Research Council Canada Institute for Aerospace Research (NRC-IAR).

2. Architecture of the controlled structure

To achieve the aerodynamic imposed purpose in the project, a first phase of the studies involved the determination of some optimized airfoils available for 35 different flow conditions (five Mach numbers and seven angles of attack combinations). The optimized airfoils were derived from a laminar WTEA-TE1 reference airfoil (Khalid & Jones, 1993 a; Khalid & Jones, 1993 b), and were used as a starting point for the actuation system design.

The chosen wing model was a rectangular one, with a chord of 0.5 m and a span of 0.9 m. The model was equipped with a flexible skin made of composite materials (layers of carbon and Kevlar fibers in a resin matrix) morphed by two actuation lines (Fig. 1). Each of our actuation lines uses three shape memory alloys wires (1.8 m in length) as actuators, connected to a current controllable power supply. Also, each line contains a cam, which moves in translation relative to the structure. The cam causes the movement of a rod related

on the roller and on the skin. The recall used is a gas spring. So, when the SMA is heating the actuator contracts and the cam moves to the right, resulting in the rise of the roller and the displacement of the skin upwards. In contrast, the cooling of the SMA results in a movement of the cam to the left, and thus a movement of the skin down. The horizontal displacement of each actuator is converted into a vertical displacement at a rate 3:1 (results a cam factor c_f=1/3). From the optimized airfoils, an approximately 8 mm maximum vertical displacement was obtained for the rods, so, a 24 mm maximum horizontal displacement should be actuated.

In the same time, 32 pressure sensors (16 optical sensors and 16 Kulite sensors), were disposed on the flexible skin in different positions along of the chord. The sensors are positioned on two diagonal lines at an angle of 15 degrees from centreline (Fig. 2). The rigid lower structure was made from Aluminium, and was designed to allow space for the actuation system and wiring (Fig. 3).
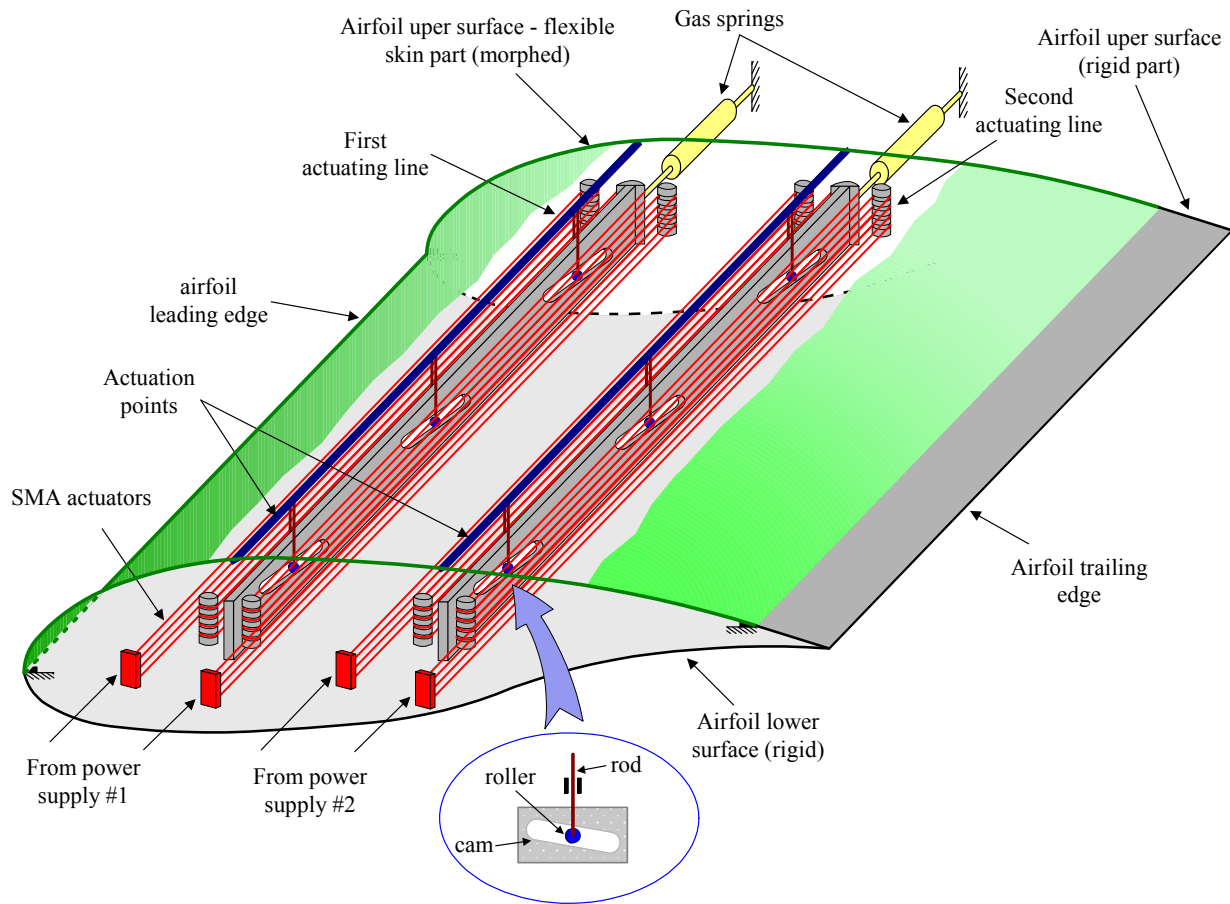

Figure 1. Model of the flexible structure.

Starting from the reference airfoil, depending on different flow conditions, 35 optimized airfoils were calculated for the desired morphed positions of the airfoil. The flow conditions were established as combinations of seven incidence angles (-1˚, -0.5˚, 0˚, 0.5˚, 1˚, 1.5˚, 2˚) and five Mach numbers (0.2, 0.225, 0.25, 0.275, 0.3). Each of the calculated optimized airfoils should be able to keep the transition point as much as possible near the trailing edge.
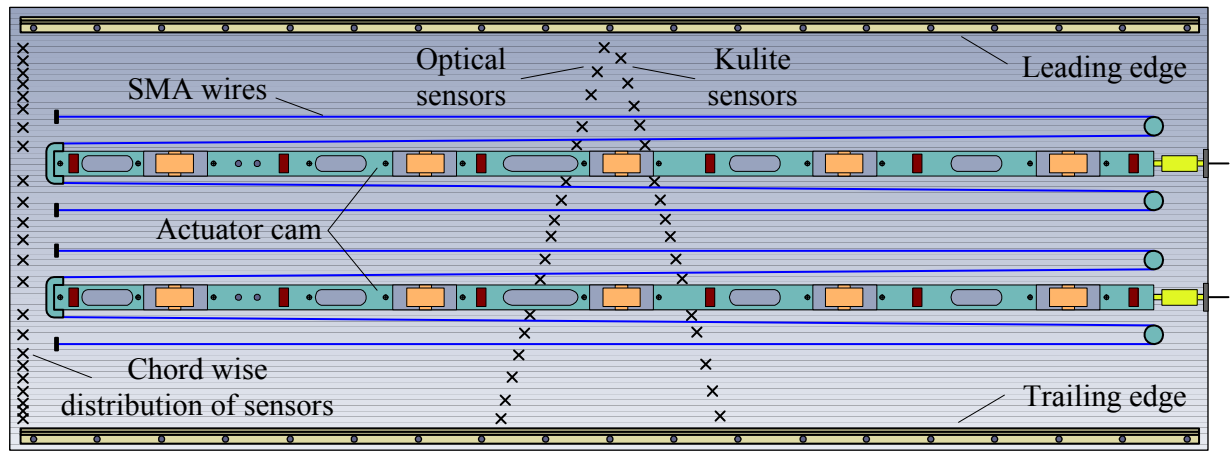
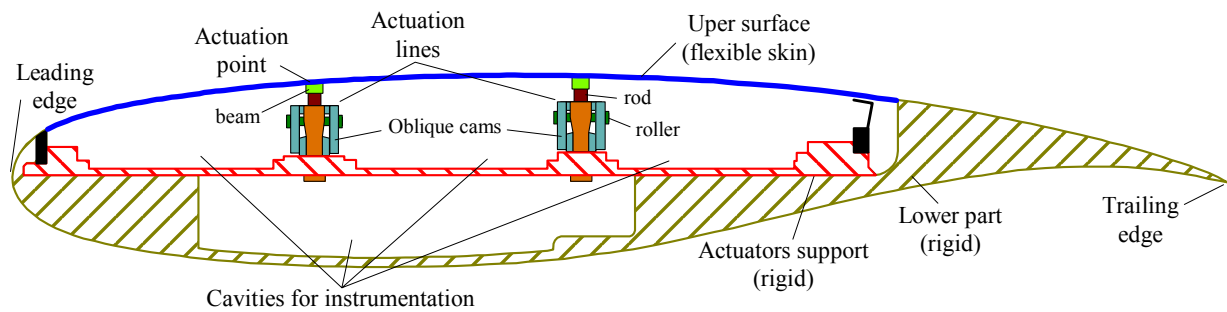**Figure 2.** Pressure sensors distribution on the flexible skin

Figure 3. Cross section of the morphing wing model.

The SMA actuator wires are made of nickel-titanium, and contract like muscles when electrically driven. Also, these have the ability to personalize the association of deflections with the applied forces, providing in this way a variety of shapes and sizes extremely useful to achieve actuation system goals. How the SMA wires provide high forces with the price of small strains, to achieve the right balance between the forces and the deformations, required by the actuation system, a compromise should be established. Therefore, the structural components of the actuation system should be designed to respect the capabilities of actuators to accommodate the required deflections and forces.

3. Open loop control of the morphing wing

For each of the two actuation lines the open loop control architecture used a controller which took as a reference value the required displacement of the actuators from a database stored in the computer memory to obtain the morphing wing optimized airfoil shape (Fig. 4); because the actuation lines' structure was identical, both of them used the same controller. As feedback signal the position signal from a linear variable differential transducer (LVDT) connected to the oblique cam sliding rod of each actuator was used. This method was called "open-loop control" due to the fact that this control method does not take direct information from the pressure sensors concerning the wind flow characteristics.
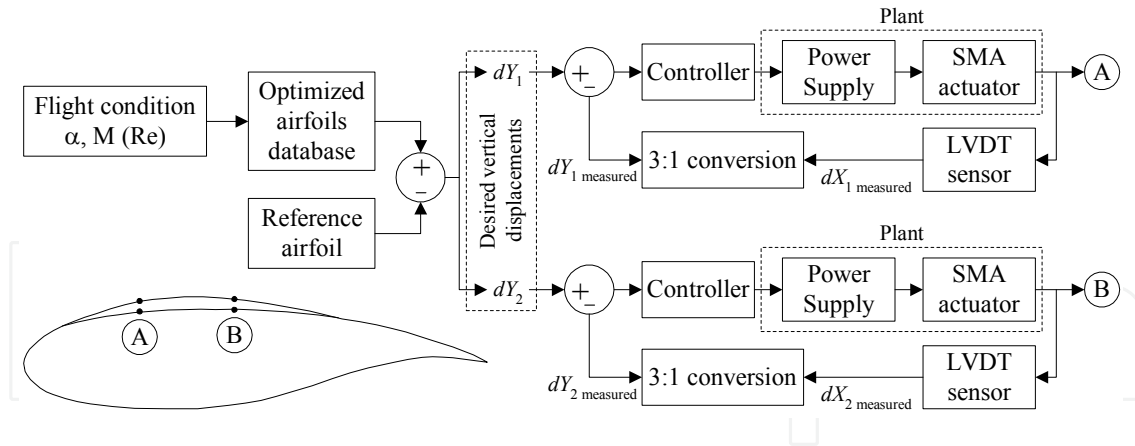
Figure 4. Open loop control architecture.

The SMA actuator control can be achieved using any method for position control. However, the specific properties of SMA actuators such as hysteresis, the first cycle effect and the impact of long-term changes must be considered.

Based on the 35 studied flight conditions, a database of the 35 optimized airfoils was built. For each flight condition, a pair of optimal vertical deflections (dY_{1opt}, dY_{2opt}) for the two actuation lines is apparent. The SMA actuators morphed the airfoil until the vertical deflections of the two actuation lines (dY_{1real}, dY_{2real}) became equal to the required deflections (dY_{1opt}, dY_{2opt}). The vertical deflections of the real airfoil at the actuation points were measured using two position transducers. The controller's role is to send a command to supply an electrical current signal to the SMA actuators, based on the error signals (*e*) between the required vertical displacements and the obtained displacements. The designed controller was valid for both actuation lines, which are practically identical.

From the point of view of the controller, the literature provides a lot of control techniques for automatic systems. The global technology evolution has triggered an ever-increasing complexity of applications, both in industry and in the scientific research fields. Many researchers have concentrated their efforts on providing simple control algorithms to cope with the increasing complexity of the controlled systems (Al-Odienat & Al-Lawama, 2008). The main challenge of a control designer is to find a formal way to convert the knowledge and experience of a system operator into a well-designed control algorithm (Kovacic & Bogdan, 2006). From another point of view, a control design method should allow full flexibility in the adjustment of the control surface, as the systems involved in practice are, generally, complex, strongly nonlinear and often with poorly defined dynamics (Al-Odienat & Al-Lawama, 2008). If a conventional control methodology, based on linear system theory, is to be used, a linearized model of the nonlinear system should have been developed beforehand. Because the validity of a linearized model is limited to a range around the operating point, no guarantee of good performance can be provided by the obtained controller. Therefore, to achieve satisfactory control of a complex nonlinear system, a nonlinear controller should be developed (Al-Odienat & Al-Lawama, 2008; Hampel et al., 2000; Kovacic & Bogdan, 2006; Verbruggen & Bruijn, 1997). From another perspective, if it would be difficult to precisely describe the controlled system by conventional mathematical

relations, the design of a controller using classical analytical methods would be totally impractical (Hampel et al., 2000; Kovacic & Bogdan, 2006). Such systems have been the motivation for developing a control system designed by a skilled operator, based on their multi-year experience and knowledge of the static and dynamic characteristics of a system; known as a Fuzzy Logic Controller (FLC) (Hampel et al., 2000). FLCs are based on fuzzy logic theory, developed by L. Zadeh (Zadeh, 1965). By using multivalent fuzzy logic, linguistic expressions in antecedent and consequent parts of IF-THEN rules describing the operator's actions can be efficiently converted into a fully-structured control algorithm suitable for microcomputer implementation or implementation with specially-designed fuzzy processors (Kovacic & Bogdan, 2006). In contrast to traditional linear and nonlinear control theory, an FLC is not based on a mathematical model, and it does provide a certain level of artificial intelligence compared to conventional PID controllers (Al-Odienat & Al-Lawama, 2008).

Due to the strong non-linear character of the smart materials actuators used in our application, one variant for the controller was developed by using the fuzzy logic techniques. We tried to counterbalance the existence of a rigorous mathematical model, a prior developed for system, avoiding in this way the loss of precision from linearization and uncertainties in the system's parameters, which negatively influences the quality of the resulting control. In the same time, we used the intuitive handling, simplicity and flexibility capabilities offered by the fuzzy logic techniques and due to their closeness to human perception and reasoning; fuzzy logic is an interface between logic an human reasoning, providing an intuitive method for describing systems in human terms and automates the conversion of those system specifications into effective models (Castellano et al., 2003; Kovacic & Bogdan, 2006; Prasad Reddy et al., 2011; Zadeh, 1965).

The controller chosen structure was a PD fuzzy logic one, having as inputs the error (difference between the desired and measured vertical displacement) and the change in error (the derivative of the error), and as output the voltage controlling the Power Supply output current (Fig. 5) (Kovacic & Bogdan, 2006). Widely accepted for capturing expert knowledge, a Mamdani controller type was used, due to its simple structure of "min-max" operations (Castellano et al., 2003).
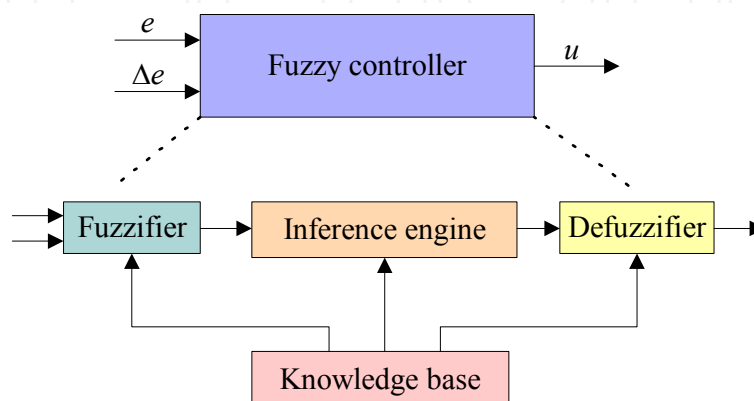

Figure 5. Fuzzy controller architecture.

The fuzzy controller internal mechanism during operation was relatively simple. On the base of the membership functions (Fig. 6), stored in the knowledge base, the fuzzifier converted the crisp inputs in linguistic variables. For our system, three membership functions were chosen for both of the two inputs (N-negative, Z-zero, P-positive), while five membership functions were considered for output (ZE-zero, PS-positive small, PM-positive medium, PB-positive big, PVB-positive very big)(Fig. 6 and Table 1); the used shape was the triangular one, defined by a lower limit a, an upper limit b, and a value m $(a \leq m \leq b)$:

$$\mu_A(x) = \begin{cases} 0, & \text{if } x \leq a \\ \dfrac{x-a}{m-a}, & \text{if } a < x \leq m \\ \dfrac{b-x}{b-m}, & \text{if } m < x < b \\ 0, & \text{if } x \geq b \end{cases} \tag{1}$$

[-1, 1] interval was considered as universe of discourse for the two inputs, while for the outputs was used [0, 1] interval.

Further, the inference engine converted the fuzzy inputs to the fuzzy output, based on the "If-Then" type fuzzy rules in Table 2.

The fuzzified inputs were applied to the antecedents of the fuzzy rules by using the fuzzy operator "AND"; in this way was obtained a single number, representing the result of the antecedent evaluation. To obtain the output of each rule, the antecedent evaluation was applied to the membership function of the consequent and the clipping (alpha-cut) method was used; each consequent membership function was cut at the level of the antecedent truth. Unifying the outputs of all eight rules, the aggregation process was performed and a fuzzy set resulted for the output variable.

mf/ parameter	Input 1 (e)			Input 2 (Δe)			Output (u)				
	$mf1$	$mf2$	$mf3$	$mf1$	$mf2$	$mf3$	$mf1$	$mf2$	$mf3$	$mf4$	$mf5$
a	-1	-1	0	-1	-0.5	0	0	0.1	0.3	0.6	0.8
m	-1	0	1	-1	0	1	0	0.25	0.5	0.75	1
b	0	1	1	0	0.5	1	0.1	0.4	0.7	0.9	1

Table 1. Parameters of the input-output membership functions

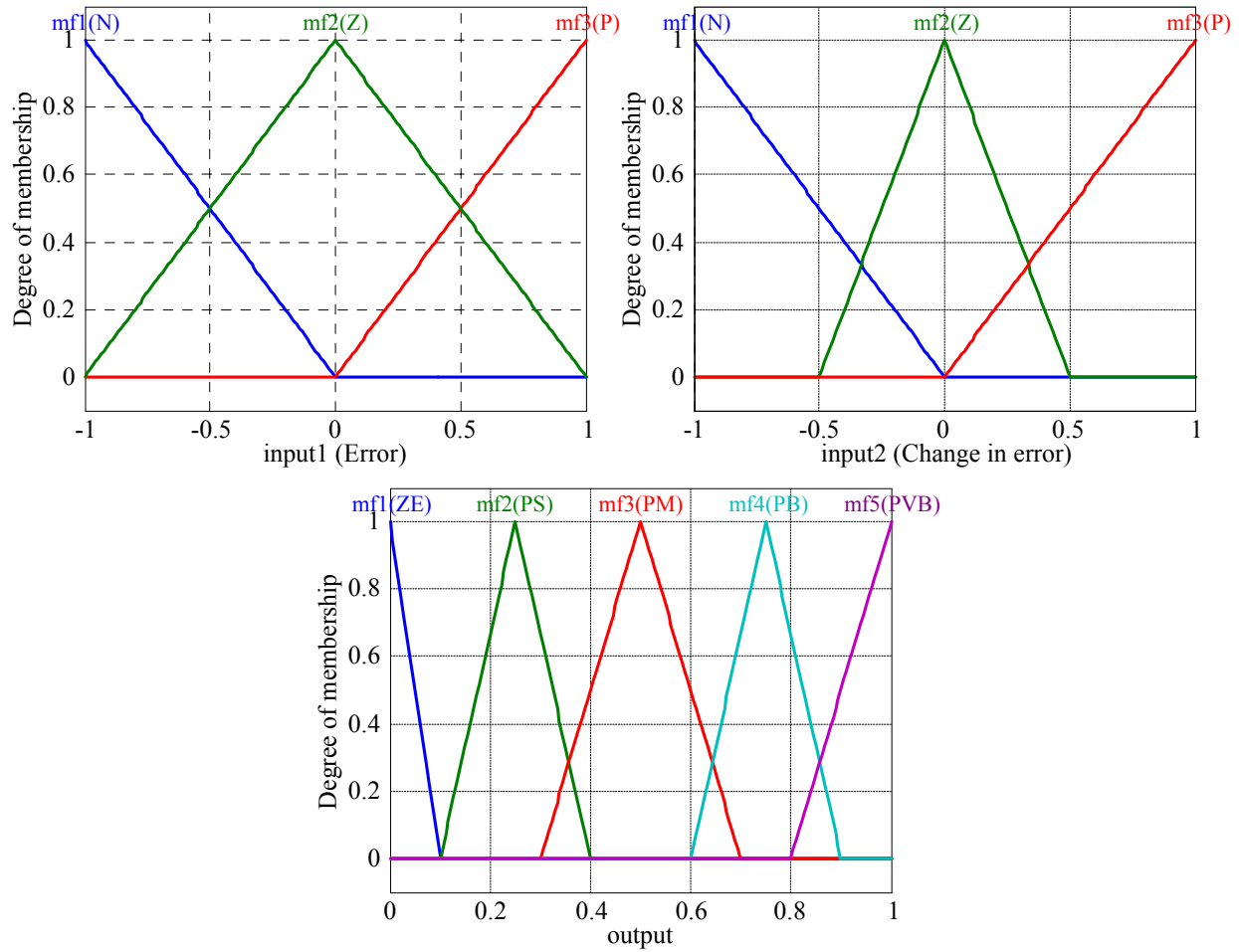| e/Δe	N	Z	P
N	ZE	ZE	ZE
Z	PS	ZE	ZE
P	PM	PVB	PB

Table 2. Inference rules

Figure 6. Membership functions

Because the output of the fuzzy system should be a crisp number, finally a defuzzification process was realized (Fig. 7); the Centroid of area (COA) method was used. The control surface resulted as in Fig. 8.

The fuzzy control surface was chosen in this way because it is normal that in the SMA cooling phase the actuators would not be powered. Therefore, the fuzzy controller was chosen to work in tandem with a bi-positional controller (particularly an on-off one). The cooling phase may occur not only when controlling a long-term phase, when a switch between two values of the actuator displacements is commended, but also in a short-lived phase, which happens when the real value of the deformation exceeds its desired value and the actuator wires need to be cooled. As a consequence, the final controller should behave as a switch between the SMA cooling and heating phases, in which the output current is 0 A, or is controlled by the fuzzy logic controller.

As a consequence, the resulted controller operational scheme can be organised as in Fig. 9.

To optimize all coefficients in the control scheme, the open loop of the morphing wing system was implemented in Matlab-Simulink model as in Fig. 10.
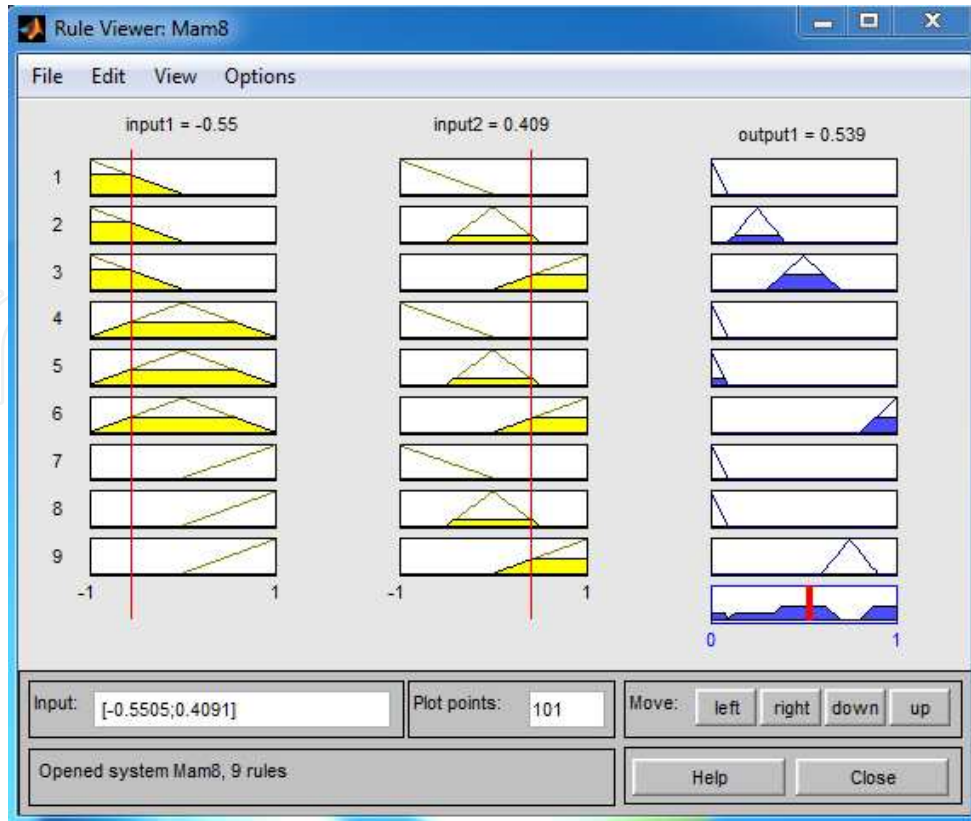
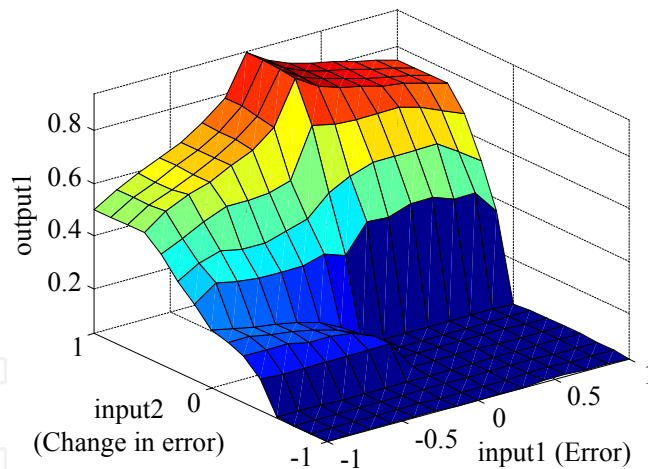**Figure 7.** Fuzzy system operating mechanism.

Figure 8. Control surface.

The "Mechanical system" block implements all the forces influencing the SMA load force: the aerodynamic force F_{aero}, the skin force F_{skin}, and the gas spring force F_{spring}; in the initialization phase, the actuators are preloaded by the gas springs even when there is no aerodynamic load applied on the flexible skin.

The "Fuzzy controller" block models the controller presented in Fig. 9. Also, SMA actuators' physical limitations in terms of temperature and supplying currents were considered in this block. Its detailed Simulink scheme is shown in Fig. 11. The block inputs are the control

error (the difference between the desired and the obtained displacements – see Fig. 9) and the SMA wires temperatures, while its output is the electrical current used to control the actuators. The first switch assured the functioning in tandem of the fuzzy controller with the on-off controller selecting one of the two options shown in Fig. 9 (error is positive or not), while the second one protected the system by switching the electrical current value to 0A when the SMA temperature value is over the imposed limit. As a supplementary protection measure, a current saturation block was used to prevent the current from going over the physical limit supported by the SMA wires.
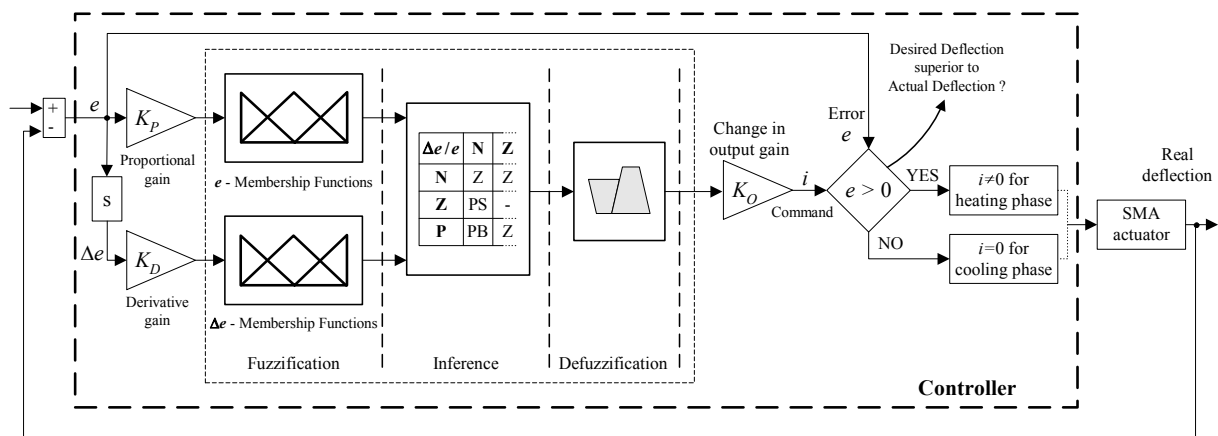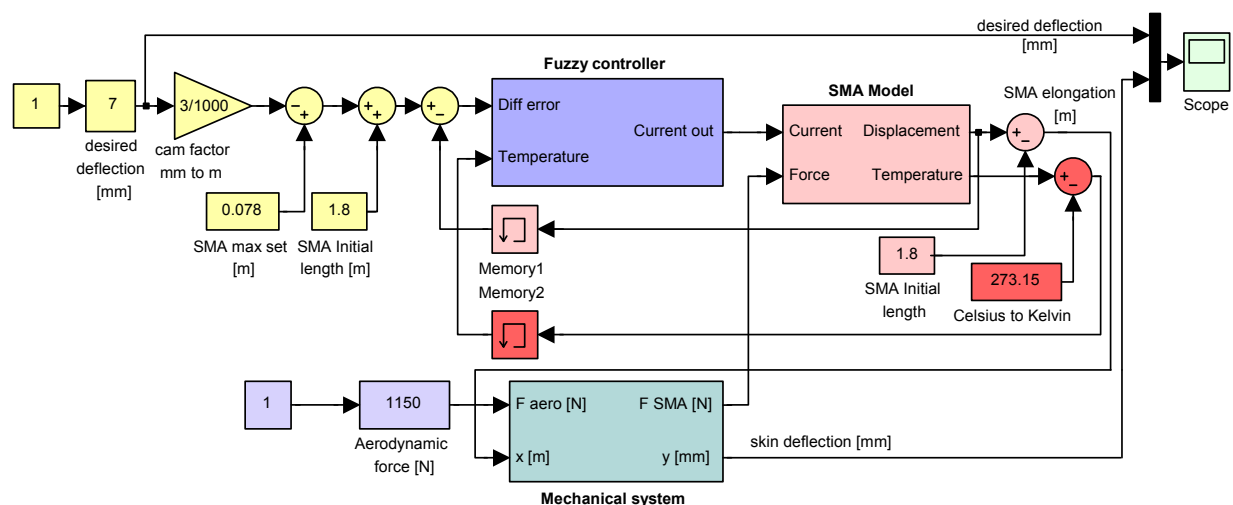

Figure 9. Operational scheme of the controller.

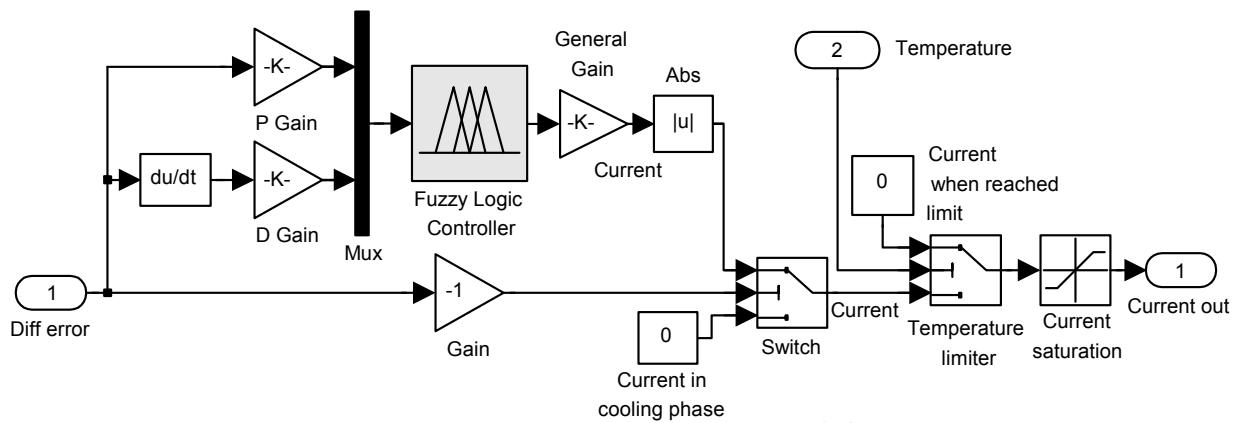**Figure 10.** Simulation model of the morphing wing system open loop.

Figure 11. "Fuzzy controller" block.

Another important block in the scheme in Fig. 10 is the „SMA model" block. This block implemented a non-linear model for the SMA actuators using a Matlab S-function. The model was built in the Shape Memory Alloys and Intelligent Systems Laboratory (LAMSI) at ETS, using Lickhatchev's theoretical model (Terriault et al., 2006).

After a tuning operation the optimum values of the gains in the scheme were established. Further, the controller was tested through numerical simulation to ensure that it works well. Fig. 12 shows the response of the actuator relative to the desired vertical displacement, the SMA actuator envelope (obtained vertical displacement vs. temperature), the SMA temperature in time, and the SMA loading force vs. temperature. Using a preliminary estimation of the forces loading the mechanical system, the next values were considered in simulations: 1150 N for aerodynamic force; 1250 N for gas spring pretension force; and the linear elastic coefficients of 2.95 N/mm and 100 N/mm, for the gas spring and for the flexible skin, respectively.

The relative allure of the obtained and desired displacements, proved the good functioning of the controller; the system's response is a critically damped one, an easier latency being observed in the cooling phase of the SMA wires in comparison with theirs heating phase. The SMAs temperature oscillations in the steady-state of the actuation position are due to theirs thermal inertia, and do not affect significantly the SMA elongation. The shape of the "displacement vs. temperature" and "loading force vs. temperature" envelopes highlights the strong nonlinear behavior of the SMA actuators.

To validate the control some experimental tests in wind tunnel were performed; all tests were performed in the IAR-NRC wind tunnel at Ottawa. The open loop experimental model is presented in Fig. 13.

According to the architecture presented in Fig. 13, the controller acted on the SMA lines by using a data acquisition card and two power supplies. The controller had also a feedback from the SMA lines behavior by using the information from two position sensors. As power supplies were chosen two Programmable Switching Power Supplies AMREL SPS100-33, while a Quanser Q8 data acquisition card was used to interface them with the control

software. The card was connected to a PC and programmed via Matlab/Simulink R2006b and WinCon 5.2. The Matlab/Simulink implemented controller received the feedback signals from two Linear Variable Differential Transformer (LVDT) potentiometers, used as position sensors to monitor the SMA wires elongations. Also, as a safety feature for the experimental model, the SMA wires temperatures were monitored and limited by the control system. Therefore, as acquisition card inputs were considered the signals from the two LVDT potentiometers and the six signals from the thermocouples installed on each of the SMA wires' components, while as outputs were considered 4 channels, used to initialize and to control each power supply through theirs analog/external control features by means of a DB-15 I/O connector.
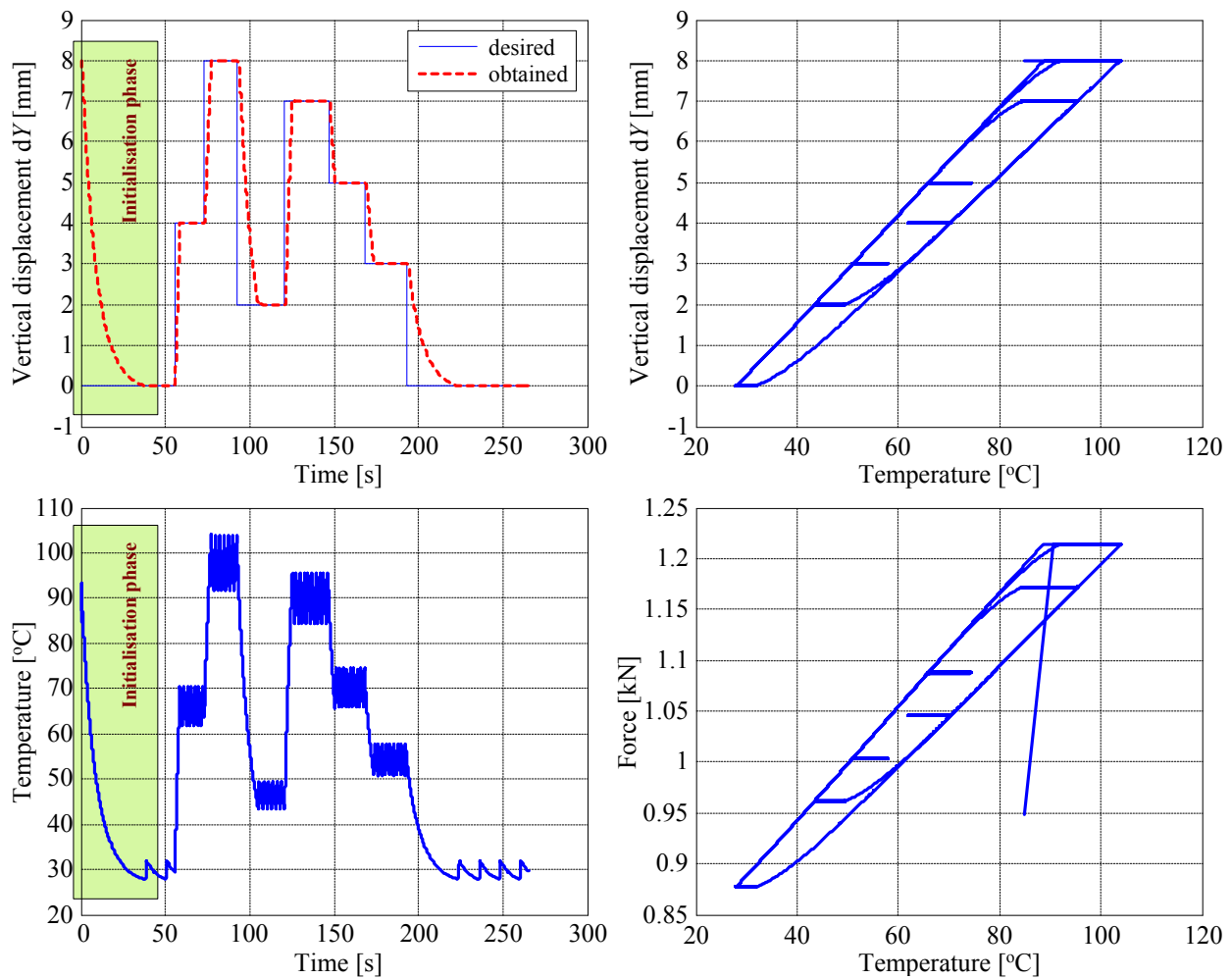

Figure 12. Numerical simulation results

In the open loop wind tunnel tests, simultaneously with the controller validation, the real-time detection and visualization of the transition point position were performed (Fig. 13), for all the thirty-five optimized airfoils; a comparative study was realized based on the transition point position estimation for the reference airfoil and for each optimized airfoil, with the aim to validate the aerodynamic part of the project. In this way, the pressure data signals obtained from the Kulite pressure sensors were used; these data were acquired using

the IAR-NRC analog data acquisition system, which was connected to the sensors. The sampling rate of each channel was at 15 kHz, which allowed a pressure fluctuation FFT spectral decomposition of up to 7.5 kHz for all channels. The signals were processed in real time using Simulink. The pressure signals were analyzed using Fast Fourier Transforms (FFT) decomposition to detect the magnitude of the noise in the surface air flow. Subsequently, the data was filtered by means of high-pass filters and processed by calculating the Root Mean Square (RMS) of the signal to obtain a plot diagram of the pressure fluctuations in the flow boundary layer. This signal processing was necessary to disparate the inherent electronically induced noise, by the Tollmien-Schlichting waves that are responsible for triggering the transition from laminar to turbulent flow. The measurements analysis revealed that the transition appeared at frequencies between 3÷5kHz and the magnitude of the pressure variations in the laminar flow boundary layer were on the order of 5e-4 Pa. The transition from the laminar flow to turbulent flow was shown by an increase in the pressure fluctuation, which was indicated by a drastic variation of the pressure signal RMS.
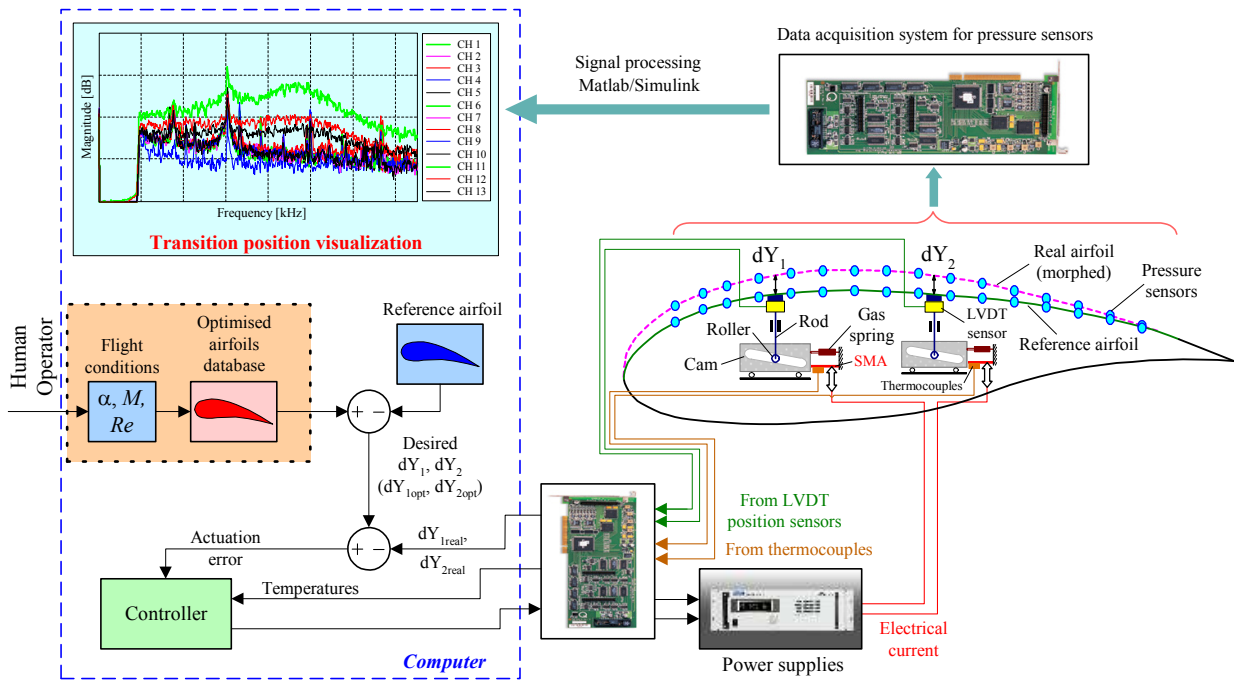

Figure 13. Architecture of the open loop morphing wing model.

In Fig. 14 are presented the results obtained for the open loop controller testing in the flow case characterized by M=0.275 and α=1.5 deg (run test 51); can be easily observed that, because of the gas springs pretension forces, the controller worked even the required vertical displacements for the actuation lines were zero millimeters. Also, some noise parasitizing the LVDT sensors measurements appeared in this test due to the wind tunnel electrical power sources and its instrumentation equipment. The transition monitoring revealed that this noise level did not influence significantly the transition point position; the positioning resolution was determined by the density of the chord-disposed pressure sensors.
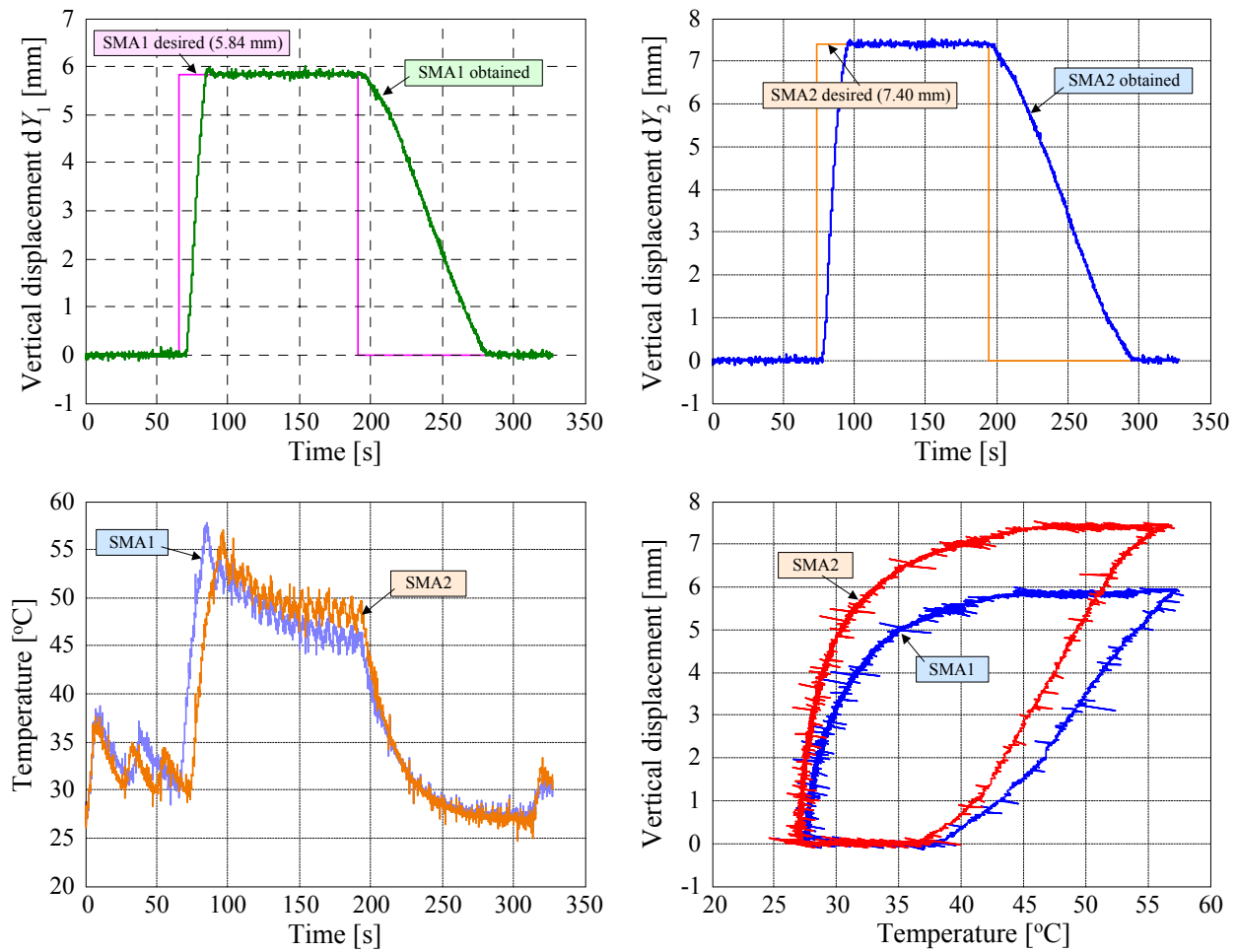
Figure 14. Wind tunnel test results for M=0.275 and α=1.5 deg flow condition.

Fig. 15 depicts the results obtained by the transition monitoring for the run test 51 (M=0.275 and α=1.5 deg); shown are the instant plots of the RMS's and spectrum for the pressure signals channels with un-morphed and morphed airfoil.

From 16 Kulite pressure sensors initially mounted on the flexible skin, only 13 channels were available (CH1 to CH13): sensor #1 was broken before the wind tunnel test, while the sensors #12 and #13 were removed from plots due to the bad dynamic signals which show electrical failure of the sensors. The left hand column presents the results for the reference (un-morphed) airfoil, and the right hand side column display the results for the optimized (morphed) airfoil. The spike of the RMS and the highest noise band on the spectral plots (CH 11 cian spectra on the right low plot) for the morphed airfoil case suggested that the flow was already turned turbulent on sensor on the channel 11 (eleventh available Kulite sensor), near the trailing edge; therefore, the transition point position was somewhere near the CH 11. For un-morphed airfoil the transition was localized by the sensor on the channel 8, with maximum RMS and the highest noise band on the spectral plots (CH 8 black spectra on the left middle plot).

The results obtained from the wind tunnel tests of open loop architecture showed that the controller performed very well in enhancing the wind aerodynamic performance.
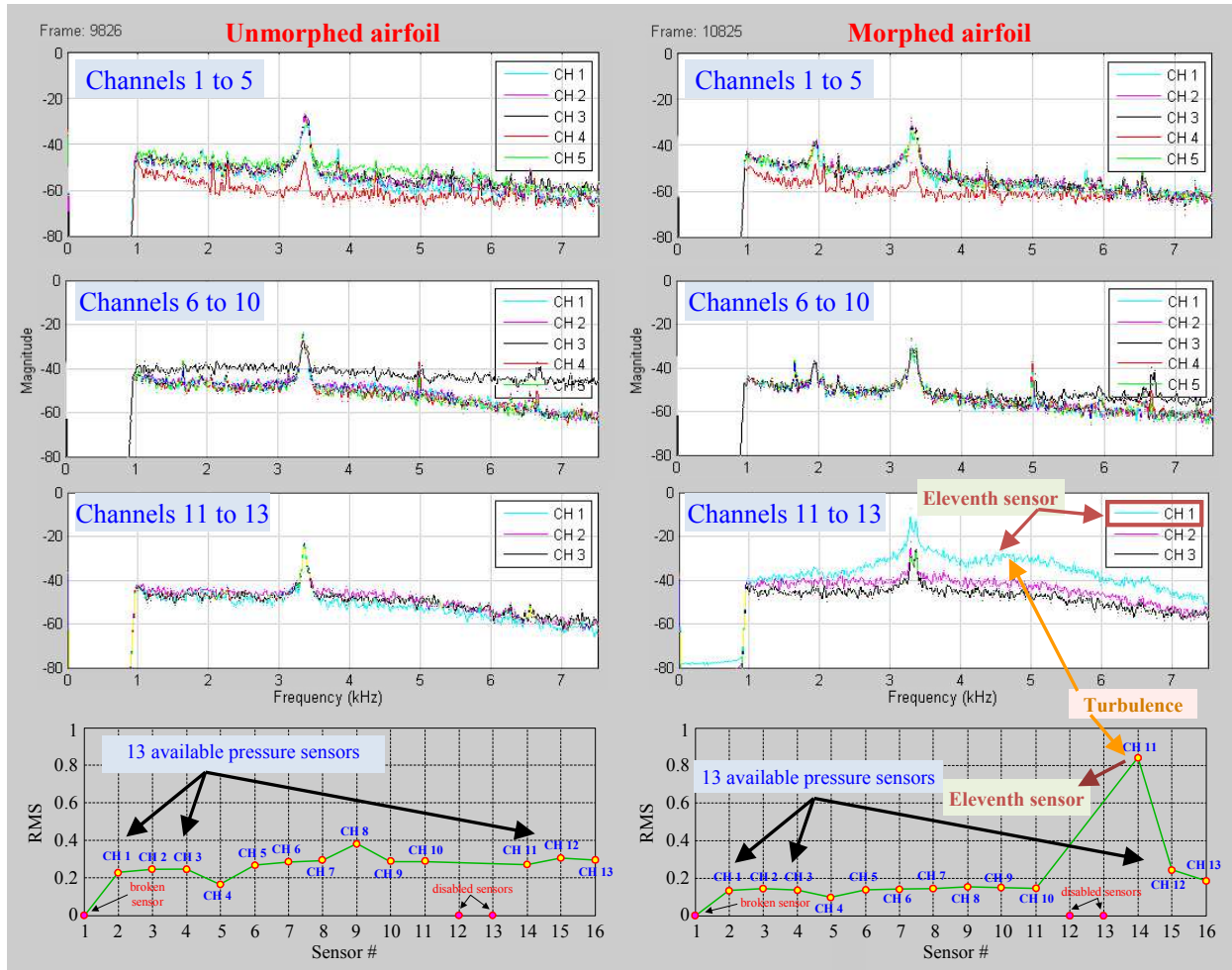

Figure 15. Transition monitoring in wind tunnel test for M=0.275 and α=1.5 deg.

4. Closed loop control of the morphing wing

The next step of the work on the morphing wing project supposed the development of the closed loop control, based on the pressure information received from the sensors and on the transition point position estimation. The closed loop control included, as inner loop, the actuation lines previous presented controller (Popov et al., 2010 a; Popov et al., 2010 b; Popov et al., 2010 c).

The closed loop architecture was developed in order to generate real time optimized airfoils starting from the information received from the pressure sensors and targeting the morphing wing main goal: the improvement of the laminar flow over the wing upper surface (Fig. 16); the previously calculated optimized airfoils database was by-passed in this control strategy, and were used just to see if the closed loop real time optimizer conducted to similar results for morphed airfoil in a flow case. To achieve the control, a mixed optimization method was used, between „the gradient ascent" or „hill climbing" method

and the „simulated annealing" method. Two variants were tested for the starting point on the optimization map control: 1) dY_1=4 mm, dY_2=4 mm (Fig. 16), and 2) dY_{1opt}, dY_{2opt} of the theoretically obtained optimized airfoil (Popov et al., 2010 a; Popov et al., 2010 b; Popov et al., 2010 c).
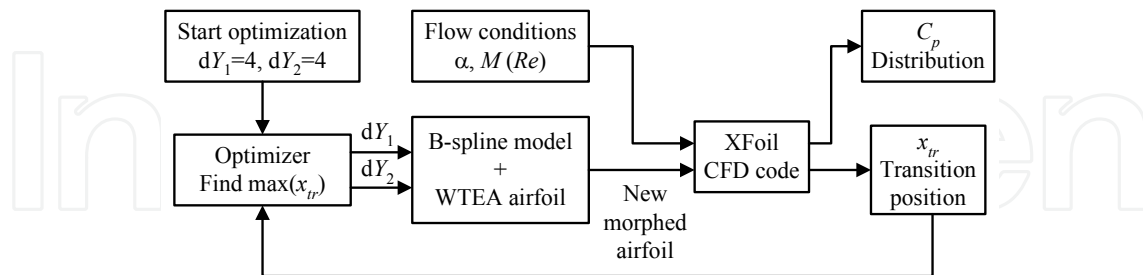

Figure 16. Optimization logic scheme for closed loop.

For the new control architecture, the software application was developed in Matlab/Simulink and two National Instruments Data Acquisition Cards were used: NI-DAQ USB 6210 and NI-DAQ USB 6229 (Quanser Q8 data acquisition card was removed from this configuration). As feedback signal for control was used the transition point position estimated starting from the pressure signals from the Kulite sensors. In the beginning of wind-tunnel tests, a number of sixteen Kulite sensors were installed, but due to their removal and re-installation during the next two wind tunnel tests, four of them were found defective. Therefore, a number of twelve sensors remained to be used during the last wind tunnel tests.

The closed loop control results and the followed optimization trajectory for α=0.5° and M=0.3 flow case are shown in Fig. 17. In this case, as starting point in optimization was used the point with the coordinates dY_{1opt} and dY_{2opt}, characterizing the theoretically obtained optimized airfoil: dY_{1opt}=4.81 mm, and dY_{2opt}=7.45 mm. The obtained rezults validated the theoretical optimized airfoil obtained by Ecole Polytechnique in Montreal for this flow case, taking into account that optimization method implemented in the closed loop conducted to a morphed airfoil almost identical with the first one (dY_{1opt_cl}=4.66 mm, and dY_{2opt_cl} =7.28 mm), and the transition was detected on the same pressure sensor with the open loop case (the tenth sensor in the array).

In Figs 18 and 19 are presented the FFTs of the Kulite pressure sensors data, and the pressure data RMSs for un-morphed (reference) and closed loop real time optimized airfoils, in this flow case. In Fig. 19 can be also observed the N factor (for transition positioning) distribution for reference airfoil and optimized airfoil. The distribution was estimated by using the XFoil computational fluid dynamics; XFoil code is free licensed software in which the e^n transition criterion is used (Drela, 2003; Drela and Giles, 1987). In these graphs, the N values calculated by XFoil for various sensors are defined by circles. In the morphed-to-optimized airfoil case, the RMS plot displayed in Fig. 19 with star symbols, showed that the sensor with the maximum RMS has become the tenth sensor plotted
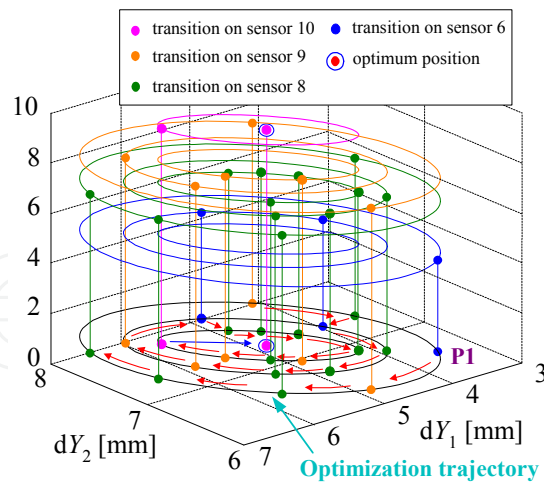
Figure 17. The closed loop real time optimization results for α=0.5° and M=0.3 flow case.

The spectral decomposition of the pressure signals in Fig. 18 confirmed the Tollmien–Schlichting wave's occurrence in the tenth sensor, visible in the highest power spectra (twelfth channel in the right hand side plots) in the frequency band of 2–5 kHz.
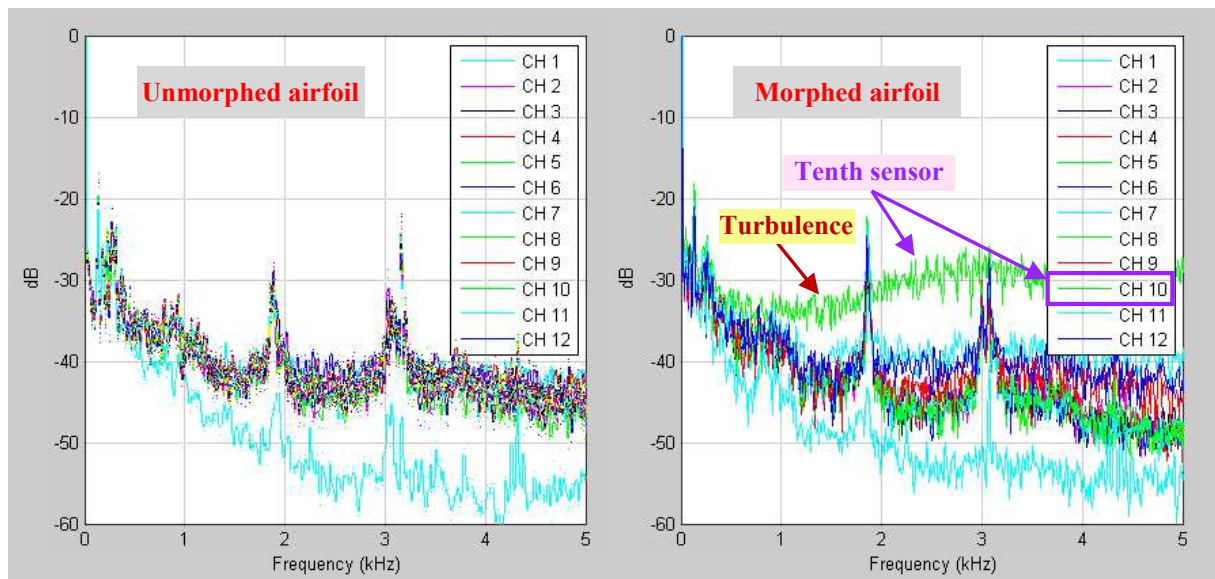

Figure 18. Pressure signals FFT for un-morphed and real time optimized airfoils, for α= 0.5° and M=0.3.
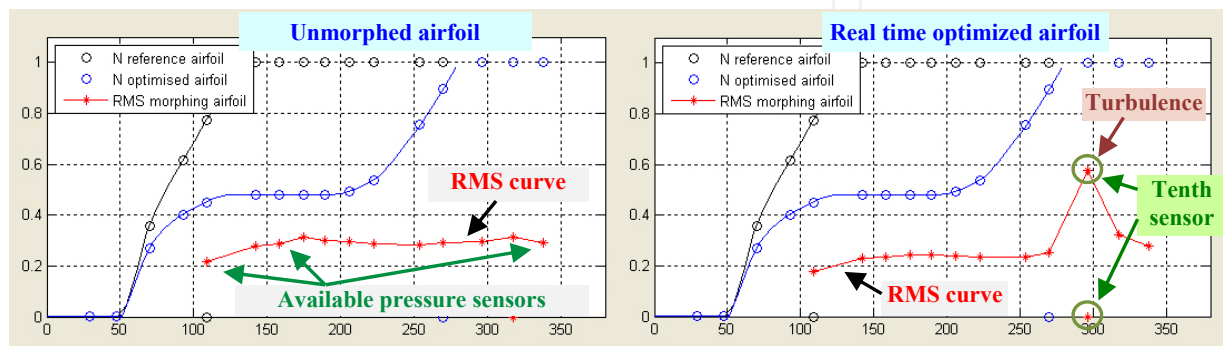

Figure 19. The pressure data RMSs and the N factor distribution

5. Conclusions

The design and validation results for an actuation system of a morphing wing were exposed. The developed morphing mechanism used smart materials such as Shape Memory Alloy (SMA) in the actuation mechanism. Two architectures were developed for the used control system: an open loop, and a closed loop one. The open loop architecture of the controller was used as an inner loop of the closed loop structure, and included a PD fuzzy logic controler in tandem with an on-off clasical controller. Both of the control architectures were validated in wind tunnel tests in parallel with the transition point real time position detection and visualization. In the closed loop controller architecture, the information about the external airflow state received from the pressure sensors system was considered and the decisions have been taken based on the transition point position estimation.

Author details

Teodor Lucian Grigorie, Ruxandra Mihaela Botez and Andrei Vladimir Popov
École de Technologie Supérieure, Canada

Acknowledgement

6. References

Ahmed, M.R.; Abdelrahman, M.M.; ElBayoumi, G. M. & ElNomrossy, M.M. (2011). Optimal wing twist distribution for roll control of MAVs, *The Aeronautical Journal*, Royal Aeronautical Society, vol. 115, 2011, pp. 641-649, ISSN: 0001-9240

Al-Odienat, A.I. & Al-Lawama, A.A. (2008). The Advantages of PID Fuzzy Controllers Over The Conventional Types, *American Journal of Applied Sciences*, Vol. 5, No. 6, pp. 653-658, June 2008, ISSN: 1546-9239

Baldelli, D.H.; Lee, D.H.; Sanchez Pena R.S. & Cannon, B. (2008). Modeling and Control of an Aeroelastic Morphing Vehicle, *Journal of Guidance, Control, and Dynamics*, Vol. 31, No. 6, November–December 2008, pp. 1687-1699, ISSN: 0731-5090

Bilgen, O.; Kochersberger, K.B. & Inman, D.J. (2009). Macro-Fiber Composite Actuators for a Swept Wing Unmanned Aircraft, *The Aeronautical Journal*, Royal Aeronautical Society, Vol. 113, 2009, pp. 385-395, ISSN: 0001-9240

Bilgen, O.; Kochersberger, K.B.; Inman, D.J. & Ohanian, O.J. (2010). Novel, Bidirectional, Variable-Camber Airfoil via Macro-Fiber Composite Actuators, *Journal of Aircraft*, Vol. 47, No. 1, January–February 2010, pp. 303-314, ISSN: 0021-8669

Bornengo, D.; Scarpa, F. & Remillat, C. (2005). Evaluation of hexagonal chiral structure for morphing airfoil concept, *Proceedings of the Institution of Mechanical Engineers, Part G: Journal of Aerospace Engineering*, 2005, vol. 219, 3, pp. 185-192, ISSN: 0954-4100

Brailovski, V.; Terriault, P.; Coutu, D.; Georges, T.; Morellon, E.; Fischer, C. & Berube, S. (2008). Morphing laminar wing with flexible extrados powered by shape memory alloy actuators, Proceedings of ASME 2008 Conference on Smart Materials, Adaptive Structures and Intelligent Systems (SMASIS2008), pp. 615-623, ISBN: 978-0-7918-4331-4, Maryland, USA, October 28–30, 2008, Publisher ASME, Ellicott City

Castellano, G.; Fanelli, A. M. & Mencar, C. (2003). Design of transparent mamdani fuzzy inference systems. In *Design and application of hybrid intelligent systems* book, IOS Print, Amsterdam, pp. 468–476, ISBN:1-58603-394-8

Coutu, D.; Brailovski, V.; Terriault, P. & Fischer, C. (2007). Experimental validation of the 3D numerical model for an adaptive laminar wing with flexible extrados, Proceedings of the 18th International Conference of Adaptive Structures and Technologies, 10 pages, Ottawa, Ontario, Canada, 3-5 October, 2007

Coutu, D.; Brailovski, V. & Terriault, P. (2009). Promising benefits of an active-extrados morphing laminar wing, *AIAA Journal of Aircraft*, Vol. 46, No. 2, pp. 730-731, March-April 2009, ISSN: 0021-8669

Drela, M. (2003). Implicit Implementation of the Full en Transition Criterion, 21st Applied Aerodynamics Conference, Orlando, Florida, 23–26 June 2003, pp. 1–8.

Drela, M. & Giles, M.B. (1987). Viscous-Inviscid Analysis of Transonic and Low Reynolds Number Airfoils, *Journal of Aircraft*, Vol. 25, No. 10, 1987, pp. 1347–1355, ISSN: 0021-8669

Gamboa, P.; Vale, J.; Lau, F. J. P. & Suleman, A. (2009). Optimization of a Morphing Wing Based on Coupled Aerodynamic and Structural Constraints, *AIAA Journal*, Vol. 47, No. 9, September 2009, pp. 2087-2104, ISSN: 0001-1452

Georges, T.; Brailovski, V.; Morellon, E.; Coutu, D. & Terriault, P. (2009). Design of Shape Memory Alloy Actuators for Morphing Laminar Wing With Flexible Extrados, *Journal of Mechanical Design*, Vol. 131, No. 9, 9 pages, 091006, September 2009, ISSN: 1050-0472

Grigorie, T.L. & Botez, R.M. (2009). Adaptive neuro-fuzzy inference system based controllers for Smart Material Actuator modeling, *Proceedings of the Institution of Mechanical Engineers, Part G: Journal of Aerospace Engineering*, Vol. 223, No. 6, pp. 655-668, June 2009, ISSN: 0954-4100

Grigorie, T.L. & Botez, R.M. (2010). New adaptive controller method for SMA hysteresis modeling of a morphing wing, *The Aeronautical Journal*, Vol. 114, No. 1151, pp. 1-13, January 2010, ISSN: 0001-9240

Grigorie, T.L.; Popov, A.V.; Botez, R.M.; Mébarki, Y. & Mamou, M. (2010 a). Modeling and testing of a morphing wing in open-loop architecture, *AIAA Journal of Aircraft*, Vol. 47, No. 3, pp. 917-923, May–June 2010, ISSN: 0021-8669

Grigorie, T. L.; Popov, A.V.; Botez, R.M.; Mamou, M. & Mebarki, Y. (2010 b). A morphing wing used shape memory alloy actuators new control technique with bi-positional and PI laws optimum combination. Part 1: design phase, Proceedings of the 7th International Conference on Informatics in Control, Automation and Robotics ICINCO 2010, pp. 5-12, ISBN: 978-989-8425-00-3, Madeira, Portugal, 15-18 June, 2010, SciTePress – Science and Technology Publications, Funchal

Grigorie, T. L.; Popov, A.V.; Botez, R.M.; Mamou, M. & Mebarki, Y. (2010 c). A morphing wing used shape memory alloy actuators new control technique with bi-positional and PI laws optimum combination. Part 2: experimental validation, Proceedings of the 7th International Conference on Informatics in Control, Automation and Robotics ICINCO 2010, pp. 13-19, ISBN: 978-989-8425-00-3, Madeira, Portugal, 15-18 June, 2010, SciTePress – Science and Technology Publications, Funchal

Hampel, R.; Wagenknecht, M. & Chaker, N. (2000). *Fuzzy Control – Theory and Practice*, Physica-Verlag, ISBN-13: 978-3790813272, USA

Inoyama, D.; Sanders, B.P. & Joo, J.J. (2008). Topology Optimization Approach for the Determination of the Multiple-Configuration Morphing Wing Structure, *Journal of Aircraft*, Vol. 45, No. 6, November–December 2008, pp. 1853-1863, ISSN: 0021-8669

Khalid, M. & Jones, D.J. (1993). Navier Stokes Investigation of Blunt Trailing Edge Airfoils using O-Grids, *AIAA Journal of Aircraft*, vol.30, no.5, pp. 797-800, 1993, ISSN: 0021-8669

Khalid, M. & Jones, D.J. (1993). A CFD Investigation of the Blunt Trailing Edge Airfoils in Transonic Flow, Inaugural Conference of the CFD Society of Canada

Kovacic, Z. & Bogdan, S. (2006). *Fuzzy Controller Design – Theory and applications*, Taylor and Francis Group, ISBN: 978-0849337475, USA

Manzo, J.; Garcia, E. & Wickenheiser, A.M. (2004) Adaptive Structural Systems and Compliant Skin Technology of Morphing Aircraft Structures, Proceedings of SPIE: The International Society for Optical Engineering, Vol. 5390, 2004, pp. 225–234

Moorhouse D.J.; Sanders B.; von Spakovsky, M.R. & Butt, J. (2006). Benefits and Design Challenges of Adaptive Structures for Morphing Aircraft, *The Aeronautical Journal*, Royal Aeronautical Society, vol. 110, 2006, pp. 157-162, ISSN: 0001-9240

Munday, D. & Jacob, J.D. (2002). Active Control of Separation on a Wing with Conformal Camber, *AIAA Journal of Aircraft*, 39, No. 1, ISSN: 0021-8669

Namgoong, H.; Crossley, W.A. & Lyrintzis, A.S. (2006). Morphing Airfoil Design for Minimum Aerodynamic Drag and Actuation Energy Including Aerodynamic Work, AIAA Paper 2006-2041, 2006, pp. 5407–5421

Namgoong, H.; Crossley, W.A. & and Lyrintzis, A.S. (2007). Aerodynamic Optimization of a Morphing Airfoil Using Energy as an Objective, *AIAA Journal*, Vol. 45, No. 9, September 2007, pp. 2113-2124, ISSN: 0001-1452

Obradovic, B. & Subbarao, K. (2011 a). Modeling of Dynamic Loading of Morphing-Wing Aircraft, *Journal of Aircraft*, Vol. 48, No. 2, March–April 2011, pp. 424-435, ISSN: 0021-8669

Obradovic, B. & Subbarao, K. (2011 b). Modeling of Flight Dynamics of Morphing-Wing Aircraft, *Journal of Aircraft*, Vol. 48, No. 2, March–April 2011, pp. 391-402, ISSN: 0021-8669

Perera, M. & Guo, S. (2009). Optimal design of an aeroelastic wing structure with seamless control surfaces, *Proceedings of the Institution of Mechanical Engineers, Part G: Journal of Aerospace Engineering*, August 1, 2009, vol. 223, 8, pp. 1141-1151, ISSN: 0954-4100

Popov, A.V.; Botez, R.M. & Labib, M. (2008 a). Transition point detection from the surface pressure distribution for controller design, *AIAA Journal of Aircraft*, Vol. 45, No. 1, pp. 23-28, January-February 2008, ISSN: 0021-8669

Popov, A.V.; Labib, M.; Fays, J. & Botez, R.M. (2008 b). Closed loop control simulations on a morphing laminar airfoil using shape memory alloys actuators, *AIAA Journal of Aircraft*, Vol. 45, No. 5, pp. 1794-1803, September-October 2008, ISSN: 0021-8669

Popov, A.V.; Botez, R.M.; Mamou, M.; Mebarki, Y.; Jahrhaus, B.; Khalid. M. & Grigorie, T.L. (2009 a). Drag reduction by improving laminar flows past morphing configurations, AVT-168 NATO Symposium on the Morphing Vehicles, 12 pages, 20-23 April, 2009, Published by NATO, Evora, Portugal

Popov, A.V.; Botez, R. M.; Mamou, M. & Grigorie, T.L. (2009 b). Optical sensor pressure measurements variations with temperature in wind tunnel testing, *AIAA Journal of Aircraft*, Vol. 46, No. 4, pp. 1314-1318, July-August 2009, ISSN: 0021-8669

Popov, A.V.; Grigorie, T. L.; Botez, R.M.; Mamou, M. & Mebarki, Y. (2010 a). Morphing wing real time optimization in wind tunnel tests, Proceedings of the 7th International Conference on Informatics in Control, Automation and Robotics ICINCO 2010, pp. 114-124, ISBN: 978-989-8425-00-3, Madeira, Portugal, 15-18 June, 2010, SciTePress – Science and Technology Publications, Funchal

Popov, A.V.; Grigorie, T. L.; Botez, R.M.; Mamou, M. & Mebarki, Y. (2010 b). Closed-Loop Control Validation of a Morphing Wing Using Wind Tunnel Tests, *AIAA Journal of Aircraft*, Vol. 47, No. 4, pp. 1309-1317, July–August 2010, ISSN: 0021-8669

Popov, A.V.; Grigorie, T. L.; Botez, R.M.; Mamou, M. & Mebarki, Y. (2010 c). Real Time Morphing Wing Optimization Validation Using Wind-Tunnel Tests, *AIAA Journal of Aircraft*, Vol. 47, No. 4, pp. 1346-1355, July–August 2010, ISSN: 0021-8669

Prasad Reddy, P.V.G.D. & Hari, Gh.V.M.K. (2011). Fuzzy Based PSO for Software Effort Estimation, International Conference on Information Technology and Mobile Communication (AIM 2011), Nagpur, India, Volume 147, Part 2, April 2011, pp. 227-232, ISSN: 1865-0929

Sainmont, C.; Paraschivoiu, I. & Coutu, D. (2009). Multidisciplinary Approach for the Optimization of a Laminar Airfoil Equipped with a Morphing Upper Surface, AVT-168 NATO Symposium on the Morphing Vehicles, 20-23 April, 2009, Published by NATO, Evora, Portugal

Sanders, B. (2003). Aerodynamic and Aeroelastic Characteristics of Wings with Conformal Control Surfaces for Morphing Aircraft, *Journal of Aircraft*, Vol. 40, No. 1, 2003, pp. 94–99, ISSN: 0021-8669

Seber, G. & Sakarya, E. (2010). Nonlinear Modeling and Aeroelastic Analysis of an Adaptive Camber Wing, *AIAA Journal of Aircraft*, Vol. 47, No. 6, November–December 2010, pp. 2067-2074, ISSN: 0021-8669

Seigler, T.M.; Neal, D.A.; Bae, J.S. & Inman, D.J. (2007). Modeling and Flight Control of Large-Scale Morphing Aircraft, *Journal of Aircraft*, Vol. 44, No. 4, July–August 2007, pp. 1077-1087, ISSN: 0021-8669

Skillen, M.D. & Crossley, W.A. (2005). Developing Response Surface Based Wing Weight Equations for Conceptual Morphing Aircraft Sizing, AIAA Paper 2005-1960, 2005, pp. 2007–2019

Terriault, P.; Viens, F. & Brailovski, V. (2006). Non-isothermal Finite Element Modeling of a Shape Memory Alloy Actuator Using ANSYS, *Computational Materials Science*, Vol. 36, No. 4, July 2006, pp. 397-410, ISSN: 0927-0256

Thill, C.; Etches, J.; Bond, I.P.; Potter, K.D. & Weaver, P.M. (2008). Morphing skins – review, *The Aeronautical Journal*, Royal Aeronautical Society, Vol. 112, 2008, pp. 117-139, ISSN: 0001-9240

Thill, C.; Downsborough, J.D.; Lai, J.S.; Bond, I.P. & Jones, D.P. (2010). Aerodynamic study of corrugated skins for morphing wing applications, *The Aeronautical Journal*, Royal Aeronautical Society, vol. 114, 2010, pp. 237-244, ISSN: 0001-9240

Verbruggen, H.B. & Bruijn, P.M. (1997). Fuzzy control and conventional control: What is (and can be) the real contribution of Fuzzy Systems?, *Fuzzy Sets Systems*, Vol. 90, No. 2, pp. 151–160, September 1997, ISSN: 0165-0114

Wildschek, A.; Havar, T. & Plötner, K. (2010). An all-composite, all-electric, morphing trailing edge device for flight control on a blended-wing-body airliner", *Proceedings of the Institution of Mechanical Engineers, Part G: Journal of Aerospace Engineering*, January 2010, vol. 224, 1, pp. 1-9, ISSN: 0954-4100

Zadeh, L.A. (1965). Fuzzy sets, *Information and Control*, Vol. 8, No. 3, pp. 339-353, June 1965, ISSN: 00199958